

## Ordered Monolayers of Free-Standing Porphyrins on Gold

Franziska L. Otte,<sup>†</sup> Sonja Lemke,<sup>‡</sup> Christian Schütt,<sup>†</sup> Nicolai R. Krekieln,<sup>‡</sup> Ulrich Jung,<sup>‡</sup> Olaf M. Magnussen,<sup>\*,‡</sup> and Rainer Herges<sup>\*,†</sup>

<sup>†</sup>Otto-Diels-Institute for Organic Chemistry and <sup>‡</sup>Institute for Experimental and Applied Physics, Christian-Albrechts-University of Kiel, 24098 Kiel, Germany

**S** Supporting Information

**ABSTRACT:** The controlled attachment of chromophores to metal or semiconducting surfaces is a prerequisite for the construction of photonic devices and artificial surface-based light-harvesting systems. We present an approach to mount porphyrins in ordered monolayers on Au(111) by self-assembly and verify it, employing STM, absorption spectroscopy, and quantum chemical calculations. The usual adsorption geometry of planar chromophores, flat on the surface or densely packed edge-on, is prevented by mounting the porphyrins upright on a molecular platform. An ethynyl unit as spacer and pivot joint provides almost free azimuthal rotation of the unsubstituted porphyrin. However, rotation of the larger triphenylporphyrin unit is sterically restricted: because the diameter of the substituted porphyrin is larger than the distance to its next neighbors, the phenyl substituents of neighboring molecules interact by dispersion force, which leads to an alignment of the azimuthal rotators.

Control of the molecular arrangement and spatial orientation of light-harvesting molecules in extended assemblies is of utmost importance in biology and the construction of a variety of artificial functional photonic devices such as organic light-emitting diodes, organic field-effect transistors, and organic photovoltaic cells in layered, bulk heterojunctions, as well as dye-sensitized solar cells.<sup>1,2</sup> In photosynthesis, well-defined aggregates of porphyrin molecules within antenna complexes are responsible for light absorption and subsequent vectorial energy transport to a chlorophyll dimer in the reaction center.<sup>3</sup> Natural<sup>4</sup> and artificial photonic devices<sup>5,6</sup> rely on precise self-organization of their components to achieve their functions. Numerous approaches were developed to assemble and to organize porphyrins into specific architectures by supramolecular<sup>7,8</sup> as well as covalent<sup>9</sup> or mixed<sup>10</sup> design. Key in the hierarchical organization of porphyrins for the construction of photonic devices is the ability to create reliably organized assemblies on conducting or semiconducting surfaces.<sup>11</sup> We describe here a method to mount porphyrins on Au(111) surfaces in well-ordered, self-assembled monolayers upright with a defined distance from the surface and to neighboring molecules as well as a uniform orientation within domains in the monolayers.

Porphyrins, phthalocyanines, and other planar chromophores readily form ordered monolayers on metal surfaces.<sup>12–14</sup> However, they tend to lie flat to maximize their dispersion interaction with the surface. Upon close contact with the metal,

photophysical<sup>15–17</sup> and coordination properties<sup>18,19</sup> change dramatically, unfortunately mostly for the worse. Excited states are efficiently quenched.<sup>20–22</sup> Their lifetimes are often too short for the energy to be used in subsequent processes such as charge separation or photoreactions.<sup>23–25</sup> Decoupling from the surface was achieved by anchoring porphyrins via spacers to the surface.<sup>11</sup> Particularly well investigated are spacers attached to a porphyrin *meso* position with one end and binding to a gold surface with a thiol terminus.<sup>26–31</sup> Four such “legs” at all *meso* positions of the porphyrin may lift the molecule somewhat, but the orientation is still parallel to the surface (Figure 1a). One or

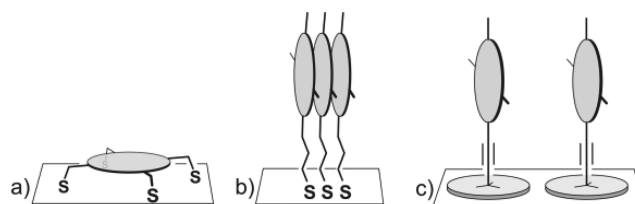


**Figure 1.** General approaches to immobilize porphyrins on gold and to decouple the chromophores electronically from the metal surface. (a) Four-leg attachment, (b) one- (or two) leg arrangement, and (c) our platform approach.

two legs lead to an upright or inclined orientation in densely packed monolayers (Figure 1b). Spacers with sufficient length indeed decouple the chromophores efficiently from the metal surface.<sup>32–34</sup> However, now another problem arises. The stacked porphyrins are in van der Waals contact and quench each other.<sup>35</sup> Bulky substituents<sup>36</sup> or coadsorption of alkane-thiols<sup>37</sup> have been used to reduce intermolecular energy transfer. Well-defined or highly ordered monolayers, however, are difficult to obtain with these methods.

To circumvent these problems, we recently developed a simple and generally applicable modular approach to mount functional molecules to metal surfaces in self-assembled monolayers.<sup>38–42</sup> Our “platform approach” allows comprehensive control of the distance and orientation to the surface and the distance to next neighbors (Figure 1c). The functional molecules stand upright in the middle of a trioxa or triaza triangulated triphenylmethane (TOTA or TATA) platform. Substituents at the nitrogen atoms control the size of the platform and thus define the distance of the platforms from each other in the densely packed hexagonal array. The carbon atom in

Received: June 3, 2014

Published: July 23, 2014

the center of the free platform is positively charged and allows the attachment of phenyl or ethynyl units as spacers in a click-type polar C–C bond formation. Different spacer types and lengths allow gradual decoupling from the surface and serve as pivot joints that allow free rotation<sup>43</sup> of the functional units on top of the spacers.<sup>44,45</sup> Ordered monolayers of these platform molecules on Au(111) substrates can be formed by simple self-assembly from solution. We have been able to prepare and to investigate well-defined SAMs with a variety of combinations of different platforms, spacers, and functional units. It is particularly important to note that azobenzenes mounted on platforms and adsorbed on gold surfaces retain their full functionality of switching from the *trans* to the *cis* isomer with UV light (365 nm) and back to the *trans* form with visible light (430 nm).<sup>46</sup> The affinity of functionalized TATA platforms to gold is mainly due to dispersion interaction. Nevertheless, the binding energy is higher than that of thiols to gold.<sup>47</sup> We report the successful preparation of self-assembled monolayers of porphyrins mounted on TATA platforms and their properties. We chose octyl-substituted TATA platforms (octyl-TATA), ethynyl spacers, and porphyrin and *meso*-triphenyl porphyrin as functional units. Ethynyl spacers were needed to provide free rotation of the porphyrins. Direct connection of the *meso* position to the TATA center would lead to severe steric hindrance of the pyrrole protons with the platform.

Octyl-TATA platforms were chosen because the distance between their centers in monolayers on gold ( $12.6 \text{ \AA}$ <sup>38,39</sup>) is larger than the diameter of unsubstituted porphyrin ( $9.2 \text{ \AA}$ ) and smaller than that of triphenyl porphyrin ( $17.9 \text{ \AA}$ ). Hence there should be almost free rotation of the small porphyrin. The larger, phenyl-substituted systems, however, should interdigitate, resulting in steric blocking of the azimuthal rotation. Therefore, not only distance and orientation to the surface and distance from each other but also orientation with respect to each other should be defined within the monolayers. Octyl-TATA was prepared according to our modified version<sup>48</sup> of Laursen and Krebs,<sup>49</sup> and ethynyl-substituted porphyrins were synthesized by the mixed aldehyde method from dipyrromethane or phenyl dipyrromethane and formaldehyde/trimethylsilylpropinal or benzaldehyde/trimethylsilylpropinal.<sup>50</sup> Coupling of the TATA platform and the silyl-protected ethynyl porphyrin was performed with powdered KOH in THF under ultrasonication (Figure 2; for details see Supporting Information).

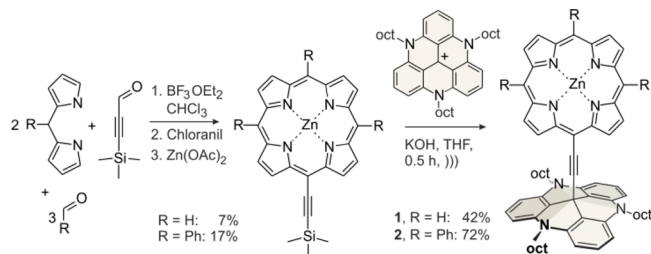


**Figure 2.** Synthesis of porphyrin-TATA **1** ( $R = \text{H}$ ) and **2** ( $R = \text{Ph}$ ).

Monolayers of **1** were prepared by 3 min immersion of Au(111) single crystals in 0.1 to 1 mM solutions of **1** in pyridine. Scanning tunneling microscopy (STM) measurements of these adsorbate layers under ambient conditions reveal a hexagonal molecular structure with distances of  $12.4 \pm 0.2 \text{ \AA}$  between neighboring molecules (Figure 3a). The pattern corresponds to a  $(\sqrt{19} \times \sqrt{19})R23.4^\circ$  superstructure, as previously observed

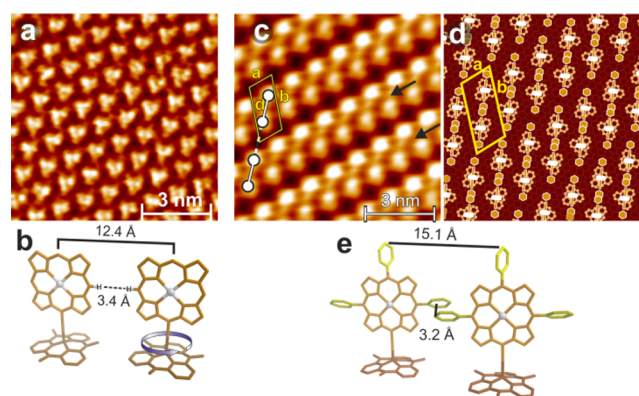


**Figure 3.** (a) STM image of porphyrin-TATA adlayer of **1** on Au(111) ( $I_t = 9 \text{ pA}$ ,  $U_{\text{Bias}} = 0.5 \text{ V}$ ). (b) DFT (PBE/SVP-D2) calculated structure of two neighboring molecules of **1**. The following restraints were applied: distance between neighboring molecules  $12.4 \text{ \AA}$  (taken from STM); only first four  $\text{CH}_2$  groups of octyl chains optimized; all platform nitrogen atoms are in a plane (constraint of the surface); orientation of porphyrins is parallel (barrier of rotation is  $0.3 \text{ kcal mol}^{-1}$ ; see Supporting Information); all other geometry parameters are optimized. (c) STM image of porphyrin-TATA adlayer of **2** on Au(111) ( $I_t = 13 \text{ pA}$ ,  $U_{\text{Bias}} = 0.48 \text{ V}$ ). (d) Structural model of the adlayer. In the unit cell (indicated by the rhombus), two molecules reside, separated by a lateral distance  $d = 15.1 \text{ \AA}$ . (e) DFT (PBE/SVP-D2) calculated structure of two neighboring molecules of **2**, at a fixed intermolecular distance of  $15.1 \text{ \AA}$  (for further restraints, see (b)).

for the bare octyl-TATA platform and for a large number of octyl-TATA derivatives with vertical functional groups of small lateral extension (e.g., phenyl, azobenzene).<sup>38,39</sup> DFT (PBE/SVP-D2) model calculations (Figure 3b; see Supporting Information for details) reveal that there is almost no barrier to azimuthal rotation of the porphyrin units. Upon rotation, the laterally extending *meso* H atoms do not come closer to each other than  $3.4 \text{ \AA}$ . Therefore, there is also no restriction to rotation by intermolecular interaction between neighboring molecules. This is in agreement with the fact that the STM image represents the three-fold symmetry of the fixed TATA platform and supports our expectations of free-standing, freely rotatable porphyrin units in this adlayer.

In contrast, adsorbate layers of **2** on Au(111), self-assembled by 1 min immersion in 0.1 to 1 mM solutions in acetonitrile, exhibit a much more complex lateral arrangement, indicating a substantial influence of the bulky triphenyl porphyrin groups on the adlayer structure. STM observations reveal characteristic double rows (Figure 3c, examples marked by arrows) with distances of  $12.9 \pm 0.4 \text{ \AA}$  between the maxima along the rows and a distance between neighboring double rows of  $26.1 \pm 0.4 \text{ \AA}$  (Figure 3c). The adlayer can be described by an oblique unit cell ( $a = 13.2 \text{ \AA}$ ,  $b = 28.8 \text{ \AA}$ ,  $\gamma = 70.9^\circ$ ), which according to the STM images is arranged on the Au(111) substrate as shown in the model in Figure 3d. The unit cell contains two maxima that are spaced at a distance  $d = 15.1 \pm 0.8 \text{ \AA}$  with respect to each other, connected by a streak of weaker apparent height. Because of its large extension, the resulting dumbbell-shaped structure cannot be assigned to a single molecule of species **2** but is attributed to a supramolecular “dimer” of two porphyrin-TATA adsorbates, formed by interactions between the lateral phenyl units of the molecules (Figure 3e) and placed on positions where all the N atoms of the TATA units occupy defined adsorption sites on the Au surface. Model calculations at the DFT level of B3LYP/6-31G\*, including dispersion interaction using the Grimme D3

method on such a dimer of **2** at a distance of 15.1 Å, reveal that the lateral phenyl substituents of neighboring porphyrins exhibit van der Waals contact and are attracting each other by dispersion interaction (for details, see Supporting Information).

These dimers form one-dimensional rows in which the porphyrin units are oriented parallel to each other. The spacing between neighboring molecules within the rows is close to the nearest neighbor spacing in a  $(\sqrt{19} \times \sqrt{19})R23.4^\circ$  structure, found for adlayers of the bare octyl-TATA platforms, suggesting that it is determined by similar packing constraints. The spacing between neighboring rows is still somewhat of a mystery. In principle, one would expect a similar interaction between the lateral phenyl groups of the molecules across the rows as within the rows (i.e., within the dimer). The significantly extended distances between molecules in adjacent rows (see dashed line in Figure 3c) indicate a more complex situation, involving a third type of supramolecular interactions. We tentatively assign those to free space requirements of the octyl side chains. While for the adlayers of **1** these alkyl chains can be accommodated in the free space between the relatively small vertical porphyrin units, the more bulky triphenyl porphyrin groups compete with those chains and thus a larger area per adsorbed molecule is required. This also reflects in the 76% lower packing density of adlayers of **2** (0.04 monolayers coverage) as compared to that of adlayers of **1** (0.053 monolayers coverage). The dimer row arrangement can be rationalized by an opposite orientation of the TATA platforms in each dimer (as indicated in Figure 3d). In this case, two of the three side chains are oriented away from the dimer rows, allowing  $\pi$ - $\pi$  interaction between the two porphyrins as well as fulfilling the space requirements of the alkane units.

Absorption spectra of the porphyrin-TATA adlayers (Figure 4), obtained in transmission mode on 10 nm thick Au films on

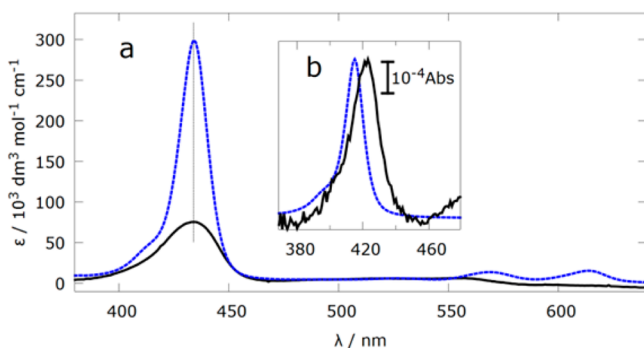


**Figure 4.** (a) UV-vis spectra of **2** in solution (blue) and 10 nm Au/quartz (black). (b) Soret band of **1** in solution (blue) and on 10 nm Au/quartz (black). The height of the Soret band of the solution spectrum is adjusted with respect to the corresponding band in the surface spectrum.

quartz (black lines), clearly show the characteristic Soret bands of the porphyrin groups. The Soret band of **2** in the monolayer at 434 nm is significantly broadened ( $\text{fwhm}_{\text{Solution}} = 15.3$  nm,  $\text{fwhm}_{\text{SAM}} = 26.4$  nm) relative to the corresponding spectra obtained for **2** in dichloromethane solution (blue line). The integrated extinction (assuming a perfect monolayer) of the Soret band is reduced to 45% compared to the solution spectrum, and the Q bands that are clearly visible in the solution spectrum of **2** at 615 and 570 nm are completely lacking in the surface spectrum. These discrepancies can be explained by a selective excitation of polarized transitions on the surface. According to TD-DFT calculations (TD-B3LYP/6-31G\*; for

details, see Supporting Information) and in agreement with qualitative MO theory, there are two Soret-type transitions with very high oscillator strengths ( $f$ ). One excitation is  $x$ -polarized ( $f = 1.5$ , orthogonal to the surface) and the other is  $y$ -polarized ( $f = 1.0$ , parallel to the surface, assuming that the molecules are standing upright, as shown in Figure 3). Upon recording of the UV-vis spectrum with a measuring beam perpendicular to the surface, the  $x$ -polarized transition is not excited because the electric field vector of the incident light beam and the transition dipole of the excitation are orthogonal. Since both Soret-type transitions are almost isoenergetic and therefore appear as a single band, the overall extinction drops to less than half if the stronger  $x$ -polarized transition is not excited. Similar selection rules hold for the Q bands. Our TD-DFT calculations predict four Q-type transitions (for details, see Supporting Information). Two excitations are  $x$ -polarized with medium oscillator strengths ( $f = 0.092$  and  $0.034$ ), and two transitions are  $y$ -polarized with low or almost zero oscillator strengths ( $f = 0.015$  and  $0.0002$ ). We therefore assign the two bands at 615 and 570 nm (blue line in Figure 4a) to the  $x$ -polarized transitions. In agreement with the selection rules (above), they are completely absent in the surface spectrum (Figure 4a, black line).

Monolayers of **1** also exhibit a slightly broadened Soret band ( $\text{fwhm}_{\text{Solution}} = 13.8$ ,  $\text{fwhm}_{\text{SAM}} = 19.3$ ), which in addition is red-shifted by 8 nm (from 415 to 423 nm) relative to the spectra in solution. Similar red shifts and broadening of the Soret band were previously reported for SAMs of other porphyrin derivatives on gold substrates<sup>36,51–53</sup> and porphyrin-containing Langmuir–Blodgett films on glass.<sup>54–56</sup> They are typically attributed to porphyrin  $\pi$ - $\pi$  interactions caused by aggregation. Specifically, it is well-established that face-to-face aggregation of the porphyrin (H-aggregates) leads to a spectral blue shift, while side-by-side aggregation (J-aggregates) leads to a red shift.<sup>6,57</sup> Following this assignment, the red shift of the Soret band in monolayers of **1** suggests a predominantly J-aggregate-like structure, whereas the broadening of the Soret band of **2** indicates a mixture of J- and H-character. The latter may be expected in view of the 2D arrangement in the adsorbate layer, where the  $\pi$ -systems of neighboring molecules are partially in-line and partially face-to-face (see Figure 3e). A quantitative treatment using the exciton model of coupled electronic transitions (Kasha's equation)<sup>58</sup> cannot be directly applied to our 2D arrangements and particularly to the freely rotating transition dipoles in **1**.

In summary, we presented a simple and efficient method to mount free-standing porphyrins in well-defined monolayers on Au(111) surfaces. The porphyrins are attached upright to molecular platforms which exhibit a high affinity to gold. Triple bonds are used as spacers and pivot joints which allow free azimuthal rotation of unsubstituted porphyrin units on the surface. Triphenyl-substituted porphyrins, which are larger than the platforms, however, are restricted in their rotation. Driven by the van der Waals interaction of the horizontal phenyl groups of neighboring porphyrins, the rotators are locked in parallel orientation. Electronic transitions that are polarized vertical to the surface are not excited, and the corresponding bands are absent in the surface UV-vis spectrum.

## ■ ASSOCIATED CONTENT

### 📄 Supporting Information

Computational details and synthetic procedures. This material is available free of charge via the Internet at <http://pubs.acs.org>.

## ■ AUTHOR INFORMATION

## Corresponding Authors

rherges@oc.uni-kiel.de  
magnussen@physik.uni-kiel.de

## Notes

The authors declare no competing financial interest.

## ■ ACKNOWLEDGMENTS

Funding by the Deutsche Forschungsgemeinschaft (SFB 677) is gratefully acknowledged.

## ■ REFERENCES

- (1) Panda, M. K.; Ladomenou, K.; Coutsolelos, A. G. *Coord. Chem. Rev.* **2012**, *256*, 2601–2627.
- (2) Jurow, M.; Schuckman, A. E.; Batteas, J. D.; Drain, C. M. *Coord. Chem. Rev.* **2010**, *254*, 2297–2310.
- (3) McDermott, G.; Prince, S. M.; Freer, A. A.; Hawthornthwaite-Lawless, A. M.; Papiz, M. Z.; Cogdell, R. J.; Isaacs, N. W. *Nature* **1995**, *374*, 517–521.
- (4) Strumpfer, J.; Sener, M.; Schulten, K. *J. Phys. Chem. Lett.* **2012**, *3*, 536–542.
- (5) Wasielewski, M. R. *Acc. Chem. Res.* **2009**, *42*, 1910–1921.
- (6) Frischmann, P. D.; Mahata, K.; Würthner, F. *Chem. Soc. Rev.* **2013**, *42*, 1847–1870.
- (7) Kobuke, Y. *Eur. J. Inorg. Chem.* **2006**, 2333–2351.
- (8) Drain, C. M.; Varotto, A.; Radivojevic, I. *Chem. Rev.* **2009**, *109*, 1630–1658.
- (9) O'Sullivan, M. C.; Sprafke, J. K.; Kondratuk, D. V.; Rinfray, C.; Claridge, T. D. W.; Saywell, A.; Blunt, M. O.; O'Shea, J. N.; Beton, P. H.; Malfois, M.; Anderson, H. L. *Nature* **2011**, *469*, 72–75.
- (10) Sprafke, J. K.; Odell, B.; Claridge, T. D. W.; Anderson, H. L. *Angew. Chem., Int. Ed.* **2011**, *50*, 5572–5575; *Angew. Chem.* **2011**, *123*, 5687–5690.
- (11) Duclairoir, F.; Marchon, J.-C. *Handb. Porphyrin Sci.* **2010**, *10*, 245–311.
- (12) Otsuki, J. *Coord. Chem. Rev.* **2010**, *254*, 2311–2341.
- (13) Ge, X.; Manzano, C.; Berndt, R.; Anger, L. T.; Köhler, F.; Herges, R. *J. Am. Chem. Soc.* **2009**, *131*, 6096–6098.
- (14) Matino, F.; Schull, G.; Jana, U.; Köhler, F.; Berndt, R.; Herges, R. *Chem. Commun.* **2010**, *46*, 6780–6782.
- (15) Sperl, A.; Kröger, J.; Berndt, R. *J. Phys. Chem. A* **2011**, *115*, 6973–6978.
- (16) Acuna, G. P.; Bucher, M.; Stein, I. H.; Steinhauer, C.; Kuzyk, A.; Holzmeister, P.; Schreiber, R.; Moroz, A.; Stefani, F. D.; Liedl, T.; Simmel, F. C.; Tinnefeld, P. *ACS Nano* **2012**, *6*, 3189–3195.
- (17) Gruyters, M.; Pingel, T.; Gopakumar, T. G.; Néel, N.; Schütt, C.; Köhler, F.; Herges, R.; Berndt, R. *J. Phys. Chem. C* **2012**, *116*, 20882–20886.
- (18) Gottfried, M.; Marbach, H. *Z. Phys. Chem.* **2009**, *223*, 53–74.
- (19) Hieringer, V.; Flechtner, K.; Kretschmann, A.; Seufert, K.; Auwärter, W.; Barth, J. V.; Görling, A.; Steinrück, H.-P.; Gottfried, J. M. *J. Am. Chem. Soc.* **2011**, *133*, 6206–6222.
- (20) Avouris, P.; Persson, B. N. J. *J. Phys. Chem.* **1984**, *88*, 837–848.
- (21) Zhang, X.-L.; Chen, L.-G.; Lv, P.; Gao, H.-Y.; Wei, S.-J.; Dong, Z.-C.; Hou, J. G. *Appl. Phys. Lett.* **2008**, *92*, 223118.
- (22) Wodtke, A. M.; Matsiev, D.; Auerbach, D. *J. Prog. Surf. Sci.* **2008**, *83*, 167–214.
- (23) Maurer, R. J.; Reuter, K. *Angew. Chem.* **2012**, *124*, 12175–12177; *Angew. Chem., Int. Ed.* **2012**, *51*, 12009–12011.
- (24) Hagen, S.; Kate, P.; Leyssner, F.; Nandi, D.; Wolf, M.; Tegeder, P. *J. Chem. Phys.* **2008**, *129*, 164102/1–8.
- (25) Yamaguchi, H.; Matsuda, K.; Irie, M. *J. Phys. Chem. C* **2007**, *111*, 3853–3862.
- (26) Kriegisch, V.; Lambert, C. *Top. Curr. Chem.* **2005**, *258*, 257–313.
- (27) Shimazu, K.; Takechi, M.; Fujii, H.; Suzuki, M.; Saiki, H.; Yoshimura, T.; Uosaki, K. *Thin Solid Films* **1996**, *273*, 250–253.
- (28) Chan, Y.-H.; Schuckman, A. E.; Pérez, L. M.; Vinodu, M.; Drain, C. M.; Batteas, J. D. *J. Phys. Chem. C* **2008**, *112*, 6110–6118.
- (29) Xue, Z.; Yang, J.; Zhi, F.; Wang, W.; Liu, X.; Lu, X. *Anal. Lett.* **2009**, *42*, 668–677.
- (30) Imahori, H.; Kashiwagi, Y.; Endo, Y.; Hanada, T.; Nishimura, Y.; Yamazaki, I.; Araki, Y.; Ito, O.; Fukuzumi, S. *Langmuir* **2004**, *20*, 73–81.
- (31) Rivas, M. V.; Mendez De Leo, L. P.; Hamer, M.; Carballo, R.; Williams, F. J. *Langmuir* **2011**, *27*, 10714–10721.
- (32) Gryko, D. T.; Clausen, C.; Lindsey, J. S. *J. Org. Chem.* **1999**, *64*, 8635–8647.
- (33) Zhu, S.-E.; Kuang, Y.-M.; Geng, F.; Zhu, J.-Z.; Wang, C.-Z.; Yu, Y.-J.; Luo, Y.; Xiao, Y.; Liu, K.-Q.; Meng, Q.-S.; Zhang, L.; Jiang, S.; Zhang, Y.; Wang, G.-W.; Dong, Z.-C.; Hou, J. G. *J. Am. Chem. Soc.* **2013**, *135*, 15794–15800.
- (34) Boeckl, M. S.; Bramblett, A. L.; Hauch, K. D.; Sasaki, T.; Ratner, B. D.; Rogers, J. W., Jr. *Langmuir* **2000**, *16*, 5644.
- (35) Hong, Y.; Lam, J. W. Y.; Tang, B. Z. *Chem. Soc. Rev.* **2011**, *40*, 5361–5388.
- (36) Imahori, V.; Norieda, H.; Nishimura, Y.; Yamazaki, I.; Higuchi, K.; Kato, N.; Motohiro, T.; Yamada, H.; Tamaki, K.; Arimura, M.; Sakata, Y. *J. Phys. Chem. B* **2000**, *104*, 1253–1260.
- (37) Thomas, K. G.; Kamat, P. V. *Acc. Chem. Res.* **2003**, *36*, 888–898.
- (38) Baisch, B.; Raffa, D.; Jung, U.; Magnussen, O. M.; Nicolas, C.; Lacour, J.; Kubitschke, J.; Herges, R. *J. Am. Chem. Soc.* **2009**, *131*, 442–443.
- (39) Kuhn, S.; Baisch, B.; Jung, U.; Johannsen, T.; Kubitschke, J.; Herges, R.; Magnussen, O. *Phys. Chem. Chem. Phys.* **2010**, *12*, 4481–4487.
- (40) Jung, U.; Kuhn, S.; Cornelissen, U.; Tuzek, F.; Strunskus, T.; Zaporozhchenko, V.; Kubitschke, J.; Herges, R.; Magnussen, O. *Langmuir* **2011**, *27*, 5899–5908.
- (41) Kuhn, S.; Jung, U.; Ulrich, S.; Herges, R.; Magnussen, O. *Chem. Commun.* **2011**, *47*, 8880–8882.
- (42) Hauptmann, N.; Scheil, K.; Gopakumar, T. G.; Otte, F. L.; Schütt, C.; Herges, R.; Berndt, R. *J. Am. Chem. Soc.* **2013**, *135*, 8814–8817.
- (43) Commins, P.; Garcia-Garibay, A. *J. Org. Chem.* **2014**, *79*, 1611–1619.
- (44) Padmaja, K.; Youngblood, W. J.; Wei, L.; Bocian, D. F.; Lindsey, J. S. *Inorg. Chem.* **2006**, *45*, 5479–5492.
- (45) Ng, D. K. P.; Jiang, J. *Chem. Soc. Rev.* **1997**, *26*, 433–441.
- (46) Jung, U.; Schütt, C.; Filinova, O.; Kubitschke, J.; Herges, R.; Magnussen, O. *J. Phys. Chem. C* **2012**, *116*, 25943–25948.
- (47) Schütt, C. Diplomarbeit, Universität Kiel, 2011.
- (48) Kubitschke, J.; Näther, C.; Herges, R. *Eur. J. Org. Chem.* **2010**, 5041–5055.
- (49) Laursen, B. W.; Krebs, F. C. *Chem.—Eur. J.* **2001**, *7*, 1773–1783.
- (50) Yamada, H.; Kushibe, K.; Okujima, T.; Uno, H.; Ono, N. *Chem. Commun.* **2006**, 383–385 (supporting information).
- (51) Imahori, H.; Norieda, H.; Ozawa, S.; Ushida, K.; Yamada, H.; Azuma, T.; Tamaki, K.; Sakata, Y. *Langmuir* **1998**, *14*, 5335–5338.
- (52) Uosaki, K.; Kondo, T.; Zhang, X.-Q.; Yanagida, M. *J. Am. Chem. Soc.* **1997**, *119*, 8367–8368.
- (53) Zak, J.; Yuan, H.; Ho, M.; Woo, L. K.; Porter, M. D. *Langmuir* **1993**, *9*, 2772–2774.
- (54) Choudhury, B.; Weedon, A. C.; Bolton, J. R. *Langmuir* **1998**, *14*, 6192–6198.
- (55) Gust, D.; Moore, T. A.; Moore, A. L.; Luttrull, D. K.; DeGraziano, J. M.; Boldt, N. J. *Langmuir* **1991**, *7*, 1483–1490.
- (56) Dick, H. A.; Bolton, J. R.; Picard, G.; Munger, G.; Leblanc, R. M. *Langmuir* **1988**, *4*, 133–136.
- (57) Kroon, J. M.; Koehorst, R. B. M.; van Dijk, M.; Sanders, G. M.; Sudhölter, E. J. R. *J. Mater. Chem.* **1997**, *7*, 615–624.
- (58) Kasha, M.; Rawls, H. R.; El-Bayoumi, M. A. *Pure Appl. Chem.* **1965**, *11*, 371–392.